MORPHOMETRY OF WRINKLE RIDGES, SOUTHERN EISTLA REGIO, VENUS. E. M. Bethell[1], R. E. Ernst[1,2], and C. Samson[1,3], [1]Department of Earth Sciences, Carleton University, Ottawa, Canada; erin-bethell@cmail.carleton.ca, [2]Faculty of Geology and Geography, Tomsk State University, Tomsk, Russia, [3]Department of Construction Engineering, École de Technologie Supérieure, Montréal, Canada.

Introduction: Wrinkle ridges are positive topographical lineaments that are found on the surfaces of all of the terrestrial planets in our solar system. They are typically a few to hundreds of kilometres in length and sinuous along their strike. Most models of wrinkle ridge formation maintain that these features are the surface expression of thrust faults and associated anticlines, although the specific details (e.g., fault dip, listric vs. simple planar geometry, role of faulting vs. folding, number of faults) of these models vary [e.g., 1,2,3].

Analysis of wrinkle ridge morphometry on Venus has so far been limited [4], as they are not resolvable at the horizontal resolution of the Magellan altimetry data (10-20 km). The development of a stereo-derived topography dataset [5], with horizontal resolution (1-2 km) improved by an order of magnitude, has enabled the first characterization of wrinkle ridge morphometry at a regional scale. We report morphometric measurements on a regional system of NNE-SSW trending wrinkle ridges in a study area bounded by 7°-26° E, 5° N-5° S, located to the south of central Eistla Regio and encompassing part of the V-32 (to the south) [6] and V-20 (to the north) quadrangles [7].

Methods: Mapping of wrinkle ridges was conducted using full resolution (75 m/pixel) left-looking synthetic aperture radar (SAR) images from Cycles 1 and 3 of NASA's Magellan mission. Topographic profiles using the stereo-derived topography data were then constructed perpendicular to strike, with ~5 km spacing between profiles. Wrinkle ridge height, width, and shortening were interpreted from these profiles. In order to determine wrinkle ridge shape, regional topographic trends unrelated to the ridge structure were removed. Background trends were modeled with a linear fit and subtracted from each profile, leaving detrended residual profiles. Wrinkle ridge shape was evaluated qualitatively and quantitatively; for the latter method, the degree of asymmetry and broadness were calculated using skewness and kurtosis functions, respectively, on residual profiles. Although shortening produced by fault slip and folding are related to the same mechanical process, they were treated as endmember processes and calculated separately, after [1] (Fig. 1). Due to complex regional topography, elevation offsets across wrinkle ridges cannot be assumed to result solely from faulting. Therefore, shortening due to faulting was only calculated for a subset of profiles that are located in areas with little to no background topographic gradients.

Results: A total of 503 topographic profiles were constructed across 40 wrinkle ridges. Results are reported graphically using histograms in Fig. 2, and minimum, maximum and average values are reported in Table 1. Standard deviations (SD) represent a combination of the natural variation in wrinkle ridge parameters between profiles and the resolution of the topography data. Using both qualitative and quantitative shape parameters, wrinkle ridges have been classified as symmetric (skewness values of -0.09 to 0.09) and asymmetric (skewness values of -0.09 to -3.00 (SE-verging) and 0.09 to 3.00 (NW-verging)). Secondary antiforms have also been observed along some wrinkle ridge profiles classified as asymmetric, which have been interpreted in other studies to represent backthrusts [e.g., 3,8]. The amount of shortening due to faulting increases with decreasing fault dip; using the average elevation offset of 72 m, a fault with a 30° dip produces a shortening of 128 m, whereas a fault with a 10° dip produces a shortening of 407 m.

Table 1. Morphometric parameters of wrinkle ridges studied. The number of profiles studied for each type of parameter is indicated by *n*.

Quantity	*n*	Minimum ± SD	Maximum ± SD	Average ± SD
Height (m)	503	39 ± 20	178 ± 63	87 ± 30
Width (km)	503	7 ± 1	18 ± 3	10 ± 1
Shortening (folding; m)	503	0.5 ± 0.4	12.3 ± 10.9	3.3 ± 2.4
Elevation offset (m)	30	14	203	72

Discussion: The wrinkle ridges studied are very broad and low relief features with high aspect ratios. Similarly high aspect ratios have been observed along ridge belts, a separate class of Venusian contractional structures [9]. Our calculations of shortening separating folding and faulting processes would seem to indicate that thrust faulting is the dominant process involved in wrinkle ridge formation on Venus, with folding being a more minor process. The same general observation was made by [1] about Lunar and Martian wrinkle ridges, and was interpreted to signify that these wrinkle ridges mostly represent surface-breaching

thrust faults. However, [2] showed by modeling wrinkle ridges as blind thrust faults (i.e., faults that do not breach the surface) that shortening due to folding at the surface may not accurately reflect the total shortening produced by folding; shortening at the surface is predicted to decrease with increasing fault depth. Regardless, the low observed relief of the wrinkle ridges studied implies relatively shallow thrust faulting, resembling a thin-skinned deformation style.

Conclusions: These preliminary results on the morphometric parameters of Venusian wrinkle ridges using stereo-derived topography data suggest that wrinkle ridges have heights and widths on the order of 10 km and 100 m, respectively.

Horizontal shortening due to folding at the surface appears to be relatively minor, on the order of a few metres, as opposed to the elevation offset resulting from faulting, which is estimated to be on the order of 100 m. Determining the relative roles and geometries of faulting and folding in the formation of Venusian wrinkle ridges will require more complex structural modeling.

References: [1] Golombek, M.P., et al. (1991). *Proc. of Lunar & Planet. Sci., 21,* 679-693. [2] Schultz, R.A. (2000). *JGR, 105,* 12035-12052. [3] Okubo, C.H. and Schultz, R.A. (2004). *GSA Bull., 116,* 594-605. [4] Bilotti, F.D. (1997). *PhD Thesis*. [5] Herrick, R.R. et al. (2012). *Eos, 93,* 125-126. [6] Bethell, E.M. et al. (2019). *Journ, of Maps, 15,* 474-486. [7] McGill, G.E. (2000). *USGS Map I-2637*. [8] Andrews-Hanna, J.C. (2019). *LPSC L,* Abstract 2922. [9] Williams, Z.W. et al. (2019). *VEXAG 17,* Abstract 2193.

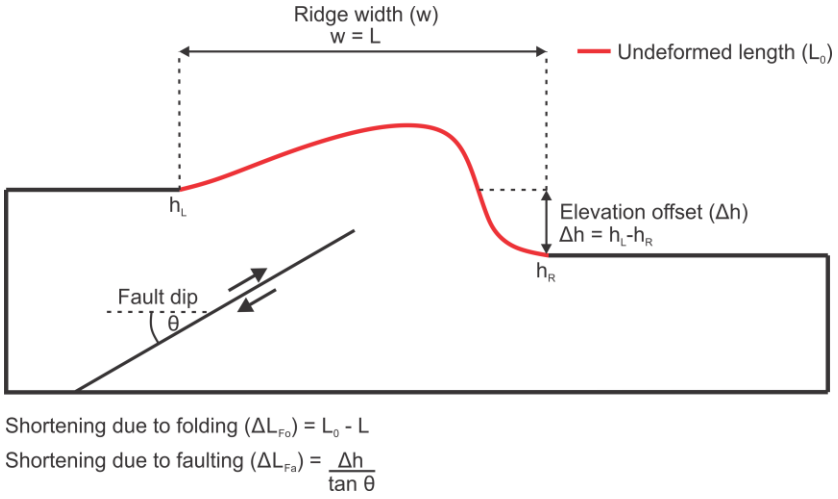

Figure 1. Schematic of a wrinkle ridge profile illustrating morphometric parameters and shortening calculations.

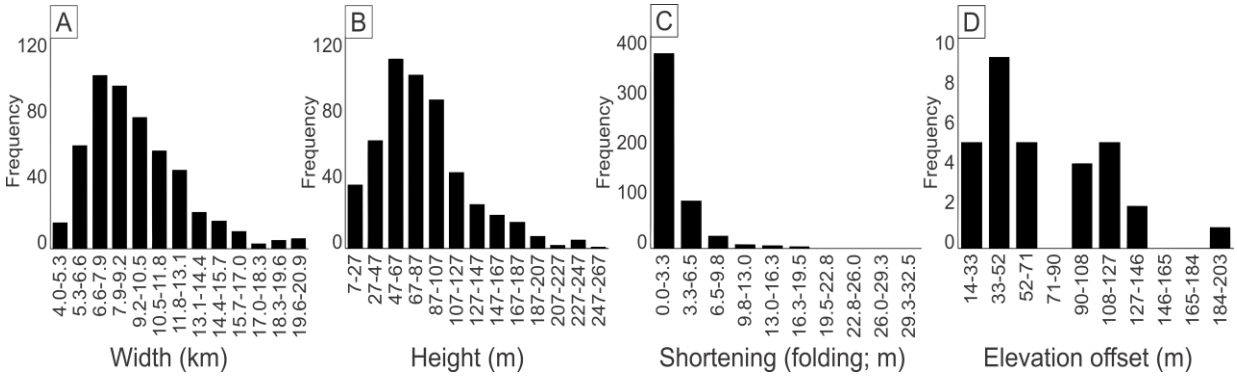

Figure 2. Histograms of parameters across the population of wrinkle ridge profiles: A) width; B) height; C) shortening due to folding; and D) elevation offset (for a subset of 30 profiles).